Optimization of 3,5-Dimethylisoxazole Derivatives as Potent Bromodomain Ligands

David S. Hewings,[†,‡] Oleg Fedorov,[‡] Panagis Filippakopoulos,[‡] Sarah Martin,[‡] Sarah Picaud,[‡] Anthony Tumber,[‡] Christopher Wells,[‡] Monica M. Olcina,[§] Katherine Freeman,[†] Andrew Gill,[∥] Alison J. Ritchie,[∥] David W. Sheppard,[∥] Angela J. Russell,[†] Ester M. Hammond,[§] Stefan Knapp,[‡] Paul E. Brennan,[‡] and Stuart J. Conway*,[†]

[†]Department of Chemistry, Chemistry Research Laboratory, University of Oxford, Mansfield Road, Oxford, OX1 3TA, U.K.

[‡]Nuffield Department of Clinical Medicine, Structural Genomics Consortium, University of Oxford, Old Road Campus Research Building, Roosevelt Drive, Oxford, OX3 3TA, U.K.

[§]Department of Oncology, Cancer Research UK/MRC Gray Institute for Radiation Oncology and Biology, University of Oxford, Old Road Campus Research Building, Oxford, OX3 7DQ, U.K.

[∥]BioFocus, Chesterford Research Park, Saffron Walden, Essex, CB10 1XL, U.K.

S *Supporting Information*

ABSTRACT: The bromodomain protein module, which binds to acetylated lysine, is emerging as an important epigenetic therapeutic target. We report the structure-guided optimization of 3,5-dimethylisoxazole derivatives to develop potent inhibitors of the BET (bromodomain and extra terminal domain) bromodomain family with good ligand efficiency. X-ray crystal structures of the most potent compounds reveal key interactions required for high affinity at BRD4(1). Cellular studies demonstrate that the phenol and acetate derivatives of the lead compounds showed strong antiproliferative effects on MV4;11 acute myeloid leukemia cells, as shown for other BET bromodomain inhibitors and genetic BRD4 knockdown, whereas the reported compounds showed no general cytotoxicity in other cancer cell lines tested.
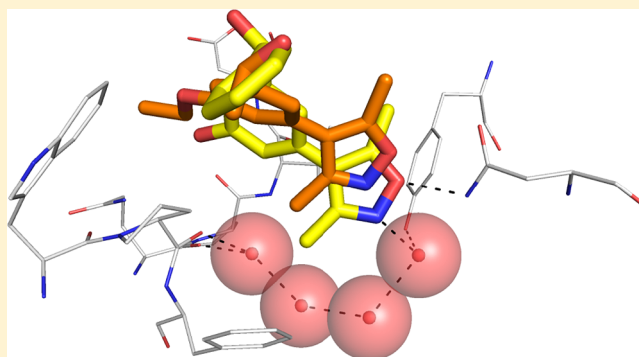
INTRODUCTION

Lysine acetylation has long been recognized as an important protein post-translation modification (PTM) that regulates a diverse array of cellular functions.[1,2] Acetylation of histone lysines, in particular, has been intensely investigated because of its key function regulating chromatin architecture and transcription.[3] Mounting evidence suggests that some histone PTMs can be maintained through multiple cell cycles, giving rise to the proposal that the specific pattern of PTMs found on histones represents a combinatorial code,[4,5] regulating gene expression. The concept of a histone code has resulted in the idea that specific protein classes exist to add the PTM marks (writer), recognize the marks (readers), and remove the marks (erasers).[3,6,7] In the case of acetylated lysine (KAc) these proteins are well characterized: histone acetyltransferases (HATs) add the acetyl group, histone deacetylases (HDACs) remove the acetyl group, and bromodomains bind to and recognize KAc, acting as "readers" of lysine acetylation state.[8,9]

There have been 61 bromodomains identified in the human proteome, which are found within 46 separate proteins, and that can be phylogenetically divided into eight distinct families.[10] The precise cellular role of most bromodomain-containing proteins (BCPs) is still unknown. However, those BCPs that have been studied in detail have been linked to certain diseases, and this work has been extensively reviewed.[3,11−15] As bromodomains are invariably components of large multidomain proteins, removal of the whole BCP does not provide information on the specific function of the bromodomain itself. Consequently, an important strategy in the study of bromodomain function is the development of small molecule probes that selectively prevent the interaction of a given bromodomain with KAc, without affecting other functions of the BCP.[6]

The most significant progress has been made in developing probes for the bromodomain and extra C-terminal domain (BET) family of bromodomains, which comprises bromodomain-containing proteins 2−4 (BRD2−4) and bromodomain testis-specific protein (BRDT).[16] The first probes identified were triazolobenzodiazepine derivatives reported by Filippakopoulos et al. (**1**)[17] and Nicodeme et al. (**2**, Figure 1).[18] The compound reported by Filippakopoulos (**1**) was based on
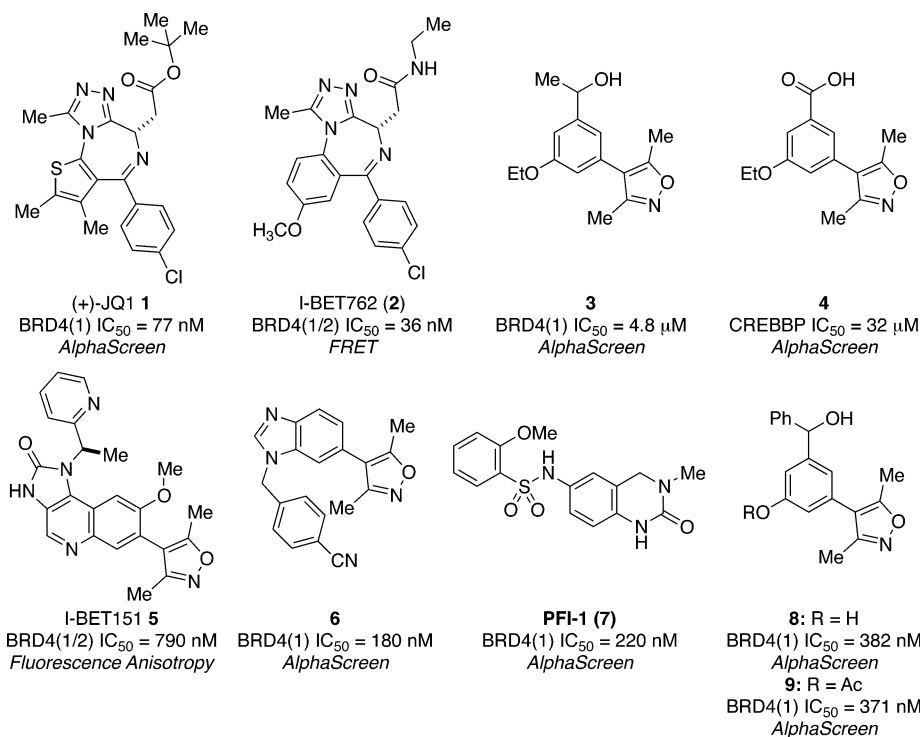
Figure 1. Structures of (+)-JQ1 (**1**),[17] I-BET762 (**2**),[18] the 3,5-dimethylisoxazoles reported by Hewings (**3**, **4**),[24] I-BET151 (**5**),[25] the 3,5-dimethylisoxazole (**6**) reported by Hay et al.,[26] PFI-1 (**7**),[27] and the optimized BET bromodomain ligands **8** and **9**. IC$_{50}$ values for the compounds are shown with the method used to obtain values given in italics. Caution must be exercised when comparing between values obtained using different methods.
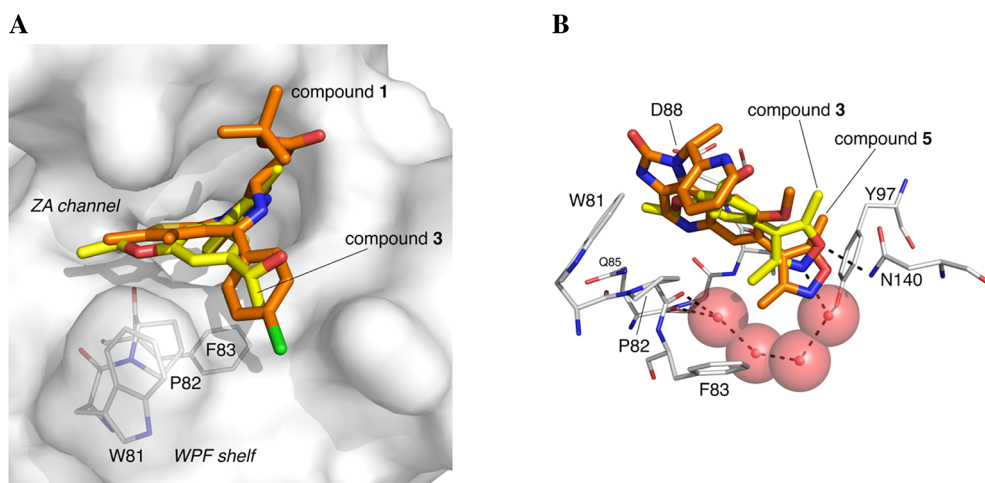

Figure 2. (A) Overlaid X-ray crystal structures of compound **3** (PDB code 3SVG, carbon = yellow)[24] and compound **1** (PDB code 3MXF, carbon = orange),[17] both bound to human BRD4(1). The methyl group of **3** does not occupy the WFP shelf as effectively as the chlorophenyl moiety of **1**. (B) Overlaid X-ray crystal structures of compound **3** (PDB code 3SVG, carbon = yellow)[24] and compound **5** (PDB code 3ZYU, carbon = orange),[25] both bound to human BRD4(1). The 3,5-dimethylisoxazole moiety of **5** resides further into the KAc-binding than that of compound **3**. Structures were aligned using the "cealign" command in PyMOL.

structures disclosed in two Mitsubishi Pharmaceuticals patents,[19,20] while the compound reported by Nicodeme et al. (**2**) was identified based on a phenotypic screen monitoring ApoA1 expression levels.[21] Further work on this chemotype has been reported by Filippakopoulos et al.[22] and Zhou et al.[23]

We[24,26] and others[25,28,29] have reported the 3,5-dimethylisoxazole moiety as an effective KAc mimic and employed it to develop a second, chemically distinct class of bromodomain ligands (**3**–**6**). We showed that compound **3** (Figure 1) binds to the BET bromodomains, having IC$_{50}$ = 4.8 μM against BRD4(1).[24] Dawson et al. also employed the 3,5-dimethylisoxazole moiety in the development of compound **5** which showed low nanomolar potency in vitro and in cell based assays.[25] Very recently a third chemotype of BET bromodomain inhibitor has been reported by Fish et al. based on the dihydroquinazolinone scaffold (**7**).[27] Herein, we detail the structure-based optimization of our previously reported lead compound (**3**)[24] to furnish potent BET bromodomain inhibitors. The affinity of the optimum compounds (**8** and **9**) was rationalized by X-ray crystallography, yielding insights into the structural require-

Scheme 1. Synthesis of the Diarylmethanol Derivatives 12−16[a]

12: X = H
13: X = m-F; 14: X = p-F
15: X = m-Cl; 16: X = p-Cl
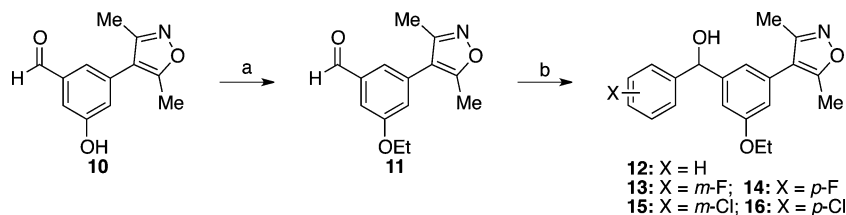
[a]Conditions: (a) EtBr, K_2CO_3, MeOH, 120 °C (microwave), 30 min, 69%. (b) X = H: PhMgBr, THF, rt, 17 h, 80%. X = m-F: 1-bromo-3-fluorobenzene, Mg, Et_2O, reflux, 2 h and then **11**, Et_2O, rt, 2 h, 92%. X = p-F: 1-bromo-4-fluorobenzene, Mg, THF, reflux, 3 h and then **11**, THF, rt, 61%. X = m-Cl: 1-bromo-3-chlorobenzene, Mg, THF, reflux, 1 h and then **11**, THF, rt, 2 h, 90%. X = p-Cl: 1-bromo-4-chlorobenzene, Mg, THF, reflux, 2.5 h and then **11**, THF, rt, 3 h, 67%.

Table 1. IC_{50} Values of Compounds 3 and 12−16 against BRD4(1) and CREBBP

Compound number	R	BRD4(1)[a] IC_{50} (μM)	CREBBP[b] IC_{50} (μM)
3	Me	4.8 (4.5-5.0)[c]	28.1 (24.4-32.5)[c]
12	Ph	0.64 (0.50-0.73)	4.1 (3.6-4.8)
13	p-F-Ph	1.5 (1.4-1.8)	8.6 (7.4-10.0)
14	m-F-Ph	1.7 (1.4-2.0)	6.3 (5.6-7.1)
15	p-Cl-Ph	2.6 (2.5-2.7)	10.8 (8.9-13.1)
16	m-Cl-Ph	3.9 (3.2-4.8)	8.5 (7.2-10.1)

[a]Protein and peptide concentration: 50 nM. [b]Protein and peptide concentration: 200 nM. Heat map shows relative IC_{50} values obtained in an ALPHA assay.[30] Red indicates low IC_{50} values, and green indicates high IC_{50} values. Ranges in parentheses represent 95% confidence intervals resulting from sigmoidal curve fitting to duplicate data. [c]Values taken from ref 24.

ments for binding to BET bromodomains and the observed SAR. In addition, compounds **8** and **9** were shown to have cellular activity consistent with a BET bromodomain inhibitor in an acute myeloid leukemia (AML) cell line.

RESULTS AND DISCUSSION

The X-ray crystal structure of our lead compound (**3**) bound to the first bromodomain of BRD4(1) showed that the methyl group bound in a shallow hydrophobic groove frequently referred as the WPF shelf (Figure 2A).[24] The ethoxy substituent was directed toward a channel formed by residues in the loop region between the Z and A helices, termed the ZA channel. In order to develop a compound with improved affinity for BRD4(1), we have investigated enhancing the interactions of the compound in these two key regions. We first chose to optimize the substituents bound in the WPF shelf. It was hypothesized that a substituent larger than the methyl group, such as those aromatic rings present in **1**, **2**, and **5**, would give an increase in BRD4(1) affinity by occupying the WPF shelf more effectively (Figure 2A). In addition, it was noted that the 3,5-dimethylisoxazole moiety of **3** binds further out of the KAc-binding pocket compared to, for example, **5** (Figure 2B). It seemed likely that the addition of a larger WPF shelf-binding substituent would push the 3,5-dimethylisoxazole further into the KAc-binding pocket, increasing interactions in this part of the protein as well. Therefore, a series of diarylmethanol derivatives (**12−16**, Scheme 1) was designed

including a simple phenyl derivative (**12**) and both meta- and para-substituted fluoro (**13** and **14**) and chloro analogues (**15** and **16**). The aldehyde **10** was a common precursor for all compounds reported here, and synthesis details are provided in the Supporting Information.

Utilizing a peptide displacement-based amplified luminescent proximity homogeneous assay (ALPHA),[24,30] we evaluated the compounds for their ability to bind the bromodomains of BRD4(1) and cAMP response element binding protein (CREB) binding protein (CREBBP) (Table 1). All compounds showed improved BRD4(1) affinity compared to the lead **3**. A clear SAR trend is evident for BRD4(1) affinity, and the simple phenyl derivative **12** is the most potent compound with an IC_{50} of 640 nM. The fluorophenyl substituents (**13** and **14**) are better tolerated than the chlorophenyl substituents (**15** and **16**), with para-substitution preferred to meta-substitution. These data suggest that increased affinity does result from a hydrophobic interaction with the WPF shelf, as has been observed with other BET bromodomain inhibitors.[16−18,29,27] It initially appears surprising that the optimum substituent in the above series of compounds is the unsubstituted phenyl ring, given that both compounds **1** and **2** possess a chlorophenyl substituent that binds in the WPF shelf region. However, it is possible that the ethoxy group that resides in the ZA channel is not optimal, pushing the aryl ring further into the WPF shelf than is the case with **1** or **2**, meaning that there is less room available for the aryl substituent to bind (Figure 2A). Our
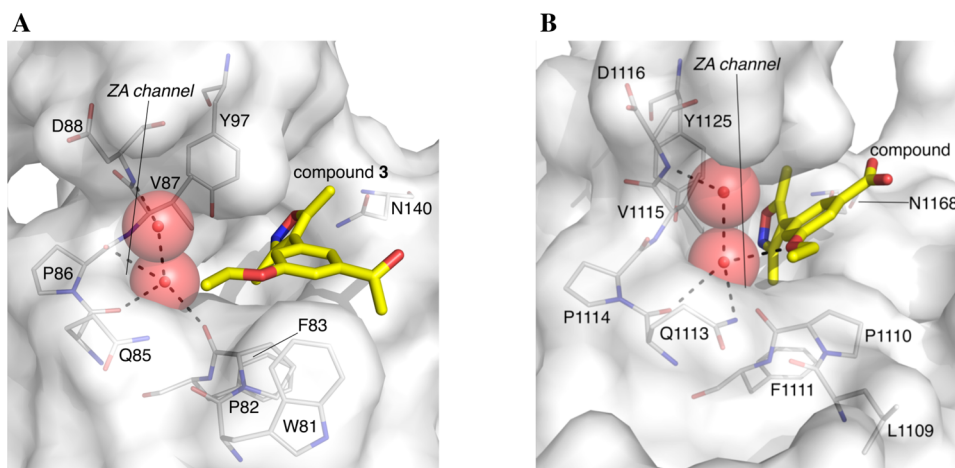
Figure 3. (A) X-ray crystal structure of compound **3** (PDB code 3SVG, carbon = yellow)[24] bound to human BRD4(1). The oxygen atom of the ethoxy group does not hydrogen bond with the ZA channel water molecules. (B) X-ray crystal structure of compound **4** (PDB code 3SVH, carbon = yellow)[24] bound to human BRD4(1). The oxygen atom of the ethoxy group forms a hydrogen bond with one of the ZA channel water molecules.

observations are consistent with the data of Bamborough et al. who synthesized sulfonamide derivatives with a range of substituents occupying the WPF shelf.[29] They noted that a lipophilic substituent of three to five heavy atoms was optimal for occupying the WPF shelf in their series of compounds. Larger substituents were tolerated but not optimal. Their series included a range of phenylsulfonamide derivatives, which would be expected to bind to the WPF shelf in a similar manner compared to compounds **12−16**; however, structural data are not available for these compounds. In their case, the *o*-chloro substituent was preferred over the *m*-chloro substituent, which was preferred over the *p*-chloro substituent. This disparity with our work might result from the phenyl rings in each series having different orientations in relation to the WPF shelf. However, the unsubstituted phenyl ring was optimal in both cases. An analogous series of methoxyphenyl-substituted sulfonamides compounds showed similar potency and trends compared to the chloro-substituted series, indicating that the electronic properties of the substituents did not affect the potency of the compound. In our case, we cannot rule out the possibility that the electron-withdrawing nature of the halide substituents is affecting the affinity of the compounds for BRD4(1).

The affinity of all compounds for the CREBBP bromodomain was also increased with compound **12** again the most potent. However, the selectivity for BRD4(1) over CREBBP was maintained, with compounds **3** and **12** both displaying approximately 6-fold selectivity for the bromodomain of BRD4(1). These data indicate that the phenyl group of **12** binds effectively to the WPF shelf region of BRD4(1), whereas interaction of this moiety with CREEBP, which does not possess this structural feature, is less favorable (see Supporting Information Figure S4). One advantage of compound **3** was its leadlike ligand efficiency of 0.39 for BRD4(1), and despite an increase in molecular weight, compound **12** retains a respectable ligand efficiency of 0.36 for BRD4(1).

The next area of SAR we wished to explore was the substituent directed toward the ZA channel. As the number of ligand-bound structures of BET bromodomains solved has increased, it has become evident that there is always one, and usually two, water molecule present in the ZA channel.[16] It was observed that in the X-ray crystal structure of compound **3**

bound to BRD4(1), the oxygen atom of the ethoxy group was not hydrogen bonding to this water molecule (Figure 3A). Conversely, an X-ray structure of a similar 3,5-dimethylisoxazole derivative (**4**) bound to the bromodomain of CREBBP was forming a hydrogen bond with the corresponding ZA channel water molecule (Figure 3B).[24] The loop region that binds the two ZA channel water molecules, which comprises P82, Q85, P86, V87, and D88 in BRD4(1), is conserved in CREBBP (P1110, Q1113, P1114, V1115, and D1116) (see Supporting Information Figure S5). It should be noted that there are some differences between the BRD4(1) and CREBBP bromodomains. Three key residues that differ are W81, K91 and D145 in BRD4(1), which correspond to L1109, L1119 and R1173 in CREBBP, respectively (see Supporting Figure S4). However, the ZA channel water molecules are bound in a very similar manner by both bromodomains, and therefore, comparison between them is valid. It seemed possible that an increase in affinity would be achieved if the ligand was able to displace, or hydrogen-bond to, one of the ZA channel water molecules.[31−34]

To test this hypothesis, compounds were designed to probe the interaction with the ZA channel water molecules. The smaller phenol (**8**) and acetate (**9**) derivatives (Scheme 2) were
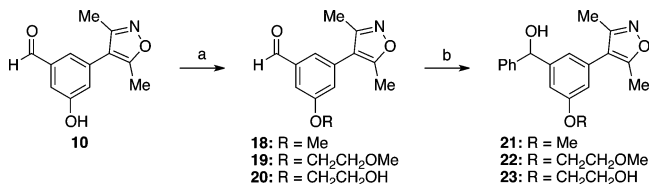
Scheme 2. Synthesis of the Phenol 8, the Acetate 9, and the Ketone 17[a]
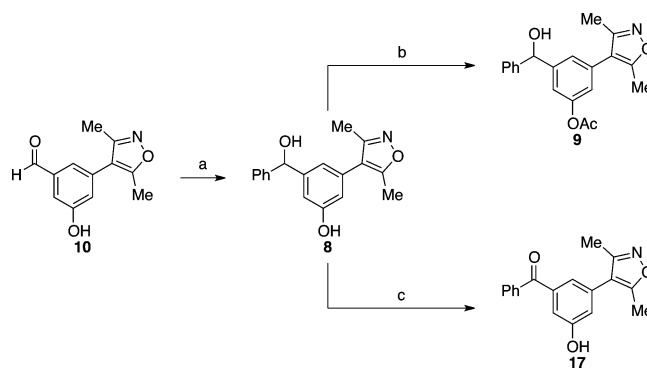
[a]Conditions: (a) PhMgBr, THF, rt, 1 h, 91%; (b) Ac$_2$O, NaOH, H$_2$O, ^{i}PrOH, rt, 1 h, 90%; (c) MnO$_2$, 1,4-dioxane, 80 °C, 53 h, 84%.

intended to form hydrogen bonds with these water molecules and hence would be expected to be the most potent if the water molecule remained in place. Larger ethylene glycol and methoxy derivatives (**21–23**, Scheme 3) were expected to be

Scheme 3. Synthesis of the Methoxy and Ethylene Glycol Derivatives (21–23)[a]

10

18: R = Me
19: R = CH$_2$CH$_2$OMe
20: R = CH$_2$CH$_2$OH

21: R = Me
22: R = CH$_2$CH$_2$OMe
23: R = CH$_2$CH$_2$OH

[a]Conditions. R = Me: (a) MeI, Cs$_2$CO$_3$, DMF, rt, 2.5 h, 92%; (b) PhMgBr, THF, 0 °C, 1 h, 76%. R = CH$_2$CH$_2$OMe: (a) 1-bromo-2-methoxyethane, K$_2$CO$_3$, MeOH, 110 °C (microwave), 30 min, 70%; (b) PhMgBr, THF, rt, 1.5 h, 83%. R = CH$_2$CH$_2$OH: (a) 2-bromoethyl acetate, Cs$_2$CO$_3$, DMF, 80 °C, 16 h and then MeOH, rt, 1.5 h, 41%; (b) PhMgBr, THF, rt, 3 h, 62%.

more potent if the water molecules were displaced. We also synthesized the ketone **17** to investigate the effect of an sp^2-hybridized carbon atom linking the two aryl rings (Scheme 2).

Compounds **8**, **9**, **17**, **21–23** were evaluated for BRD4(1) affinity in an ALPHA assay (Table 2). The phenol (**8**) and acetate (**9**) showed IC$_{50}$ values of 370–390 nM against BRD4(1), which is a significant enhancement in BRD4(1) affinity compared to the ethyl ether **12**. The ketone **17** had a slightly higher IC$_{50}$ of 544 nM. The ethylene glycol and methoxy derivatives (**21–23**) had affinities greater than 1 μM for BRD4(1). As only the (*R*)-enantiomer of the lead compound **3** was observed in its X-ray crystal structure in complex with BRD4(1), the (*R*)- and (*S*)-enantiomers of phenol **8** were separated (Supporting Information Figure S1)

and evaluated individually. Unexpectedly, both enantiomers displayed similar affinity for BRD4(1). This observation was confirmed by surface plasmon resonance using immobilized BRD4(1). K_D values of 0.36 (0.30–0.41) μM for the (*R*)-enantiomer and of 0.39 (0.37–0.40) μM for the (*S*)-enantiomer were in good agreement with those determined in the ALPHA assay and demonstrated 1:1 binding stoichiometry with rapid on and off rates (Supporting Information Table S1 and Figure S3). Compared to the lead compound (**3**), **8** maintains the ligand efficiency and improves the lipophilic ligand efficiency (Table 3). Having confirmed

Table 3. pIC$_{50}$ Values, Ligand Efficiencies, clogP Values, and Lipophilic Ligand Efficiencies for Compounds 3, (+)-8, and 9

compd	BRD4(1)[a] IC$_{50}$ (μM)	pIC$_{50}$	ligand efficiency	clogP[b]	lipophilic ligand efficiency
3	4.80	5.32	0.39	2.2	3.12
(*S*)-(+)-**8**	0.382	6.42	0.41	2.5	3.92
9	0.371	6.43	0.36	2.6	3.83

[a]Protein and peptide concentration: 50 nM. [b]clogP was calculated using ACD/Labs (algorithm version 5.0.0.184).

that the enantiomers were stable in buffer and did not racemize (Supporting Information Figure S2), we obtained X-ray crystal structures of both (*R*)-(−) and (*S*)-(+)-**8** in complex with BRD4(1) (Figure 4) in order to rationalize the observed affinities and to determine whether our SAR predictions were correct. The absolute configurations were assigned after obtaining X-ray crystal structures of the (−)- and (+)-enantiomers of **8** in complex with BRD4(1).

The X-ray crystal structures reveal that the (*R*)- and (*S*)-enantiomers have almost identical modes of binding to BRD4(1). Overlaying the X-ray crystal structures of **8** [(*S*)-**8**

Table 2. IC$_{50}$ Values of Compounds 8, 9, 17, 21–23 against BRD4(1)

8: R = H
9: R = Ac
21: R = Me
22: R = CH$_2$CH$_2$OMe
23: R = CH$_2$CH$_2$OH

17

Compound number	R	Chirality (*)	BRD4(1)[a] IC$_{50}$ (μM)	CREBBP[b] IC$_{50}$ (μM)
9	Ac	*rac*	0.371 (0.341-0.403)	2.48 (1.95-3.15)
8	H	(*S*)-(+)	0.382 (0.346-0.420)	0.771 (0.593-1.00)
8	H	(*R*)-(−)	0.386 (0.345-0.420)	1.10 (0.787-1.55)
17	H	-	0.544 (0.459-0.645)	-
23	CH$_2$CH$_2$OH	*rac*	1.17 (1.02-1.33)	2.81 (2.33-3.38)
21	Me	*rac*	1.36 (1.18-1.57)	3.96 (3.09-5.07)
22	CH$_2$CH$_2$OMe	*rac*	1.38 (1.18-1.61)	2.07 (1.58-2.72)

[a]Protein and peptide concentration: 50 nM. [b]Protein and peptide concentration: 50 nM. Heat map shows relative IC$_{50}$ values obtained in an ALPHA assay.[30] Red indicates low IC$_{50}$ values, and green/yellow indicates high IC$_{50}$ values. Ranges in parentheses represent 95% confidence intervals resulting from sigmoidal curve fitting to duplicate data.
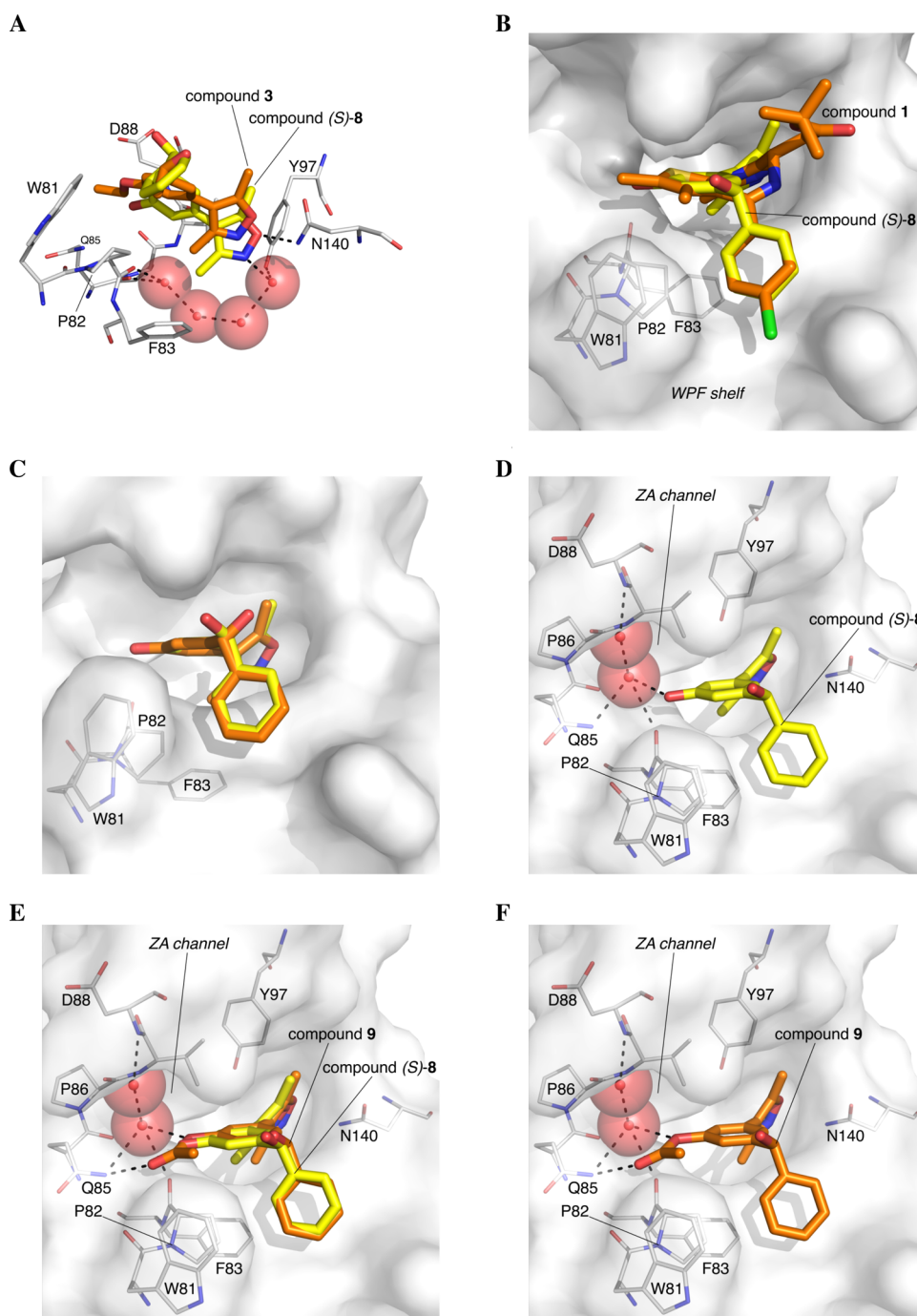
Figure 4. (A) X-ray crystal structures of compound **3** (PDB code 3SVG, carbon = orange) and (*S*)-**8** (PDB code 4J0S, carbon = yellow) both bound to human BRD4(1). The 3,5-dimethylisoxazole moiety of (*S*)-**8** resides deeper in the KAc-binding pocket than that of **3**. (B) Overlaying the X-ray crystal structure of (*S*)-**8** (PDB code 4J0S, carbon = yellow) and **1** (PDB code 3MXF, carbon = orange) demonstrates that the phenyl group of (*S*)-**8** binds to the WPF shelf in a similar position as the chlorophenyl group of **1**. (C) Overlaying the X-ray crystal structures of (*R*)-**8** (PDB code 4J0R, carbon = orange) and (*S*)-**8** (PDB code 4J0S, carbon = yellow) demonstrates that the hydroxyl group attached to the stereogenic center is solvent exposed. (D) The phenol hydroxyl group of **8** (PDB code 4J0S, carbon = yellow) forms a hydrogen bond with one of the conserved ZA channel water molecules. (E) Docking studies indicate that a feasible binding mode for **9** (docked, carbon = orange) is in a similar orientation as (*S*)-**8** (PDB code 4J0S, carbon = yellow), with the 3,5-dimethylisoxazole occupying the KAc-binding pocket and the phenyl ring residing on the WPF shelf. (F) The phenolic oxygen atom of **9** is predicted to form a hydrogen bond with one of the conserved ZA channel water molecules. The acetate carbonyl group is predicted to form a hydrogen bond with a side chain of Q85. The methyl of the acetate group is predicted to be located in a hydrophobic region close to W81.

shown] with that of **3** bound to BRD4(1) shows that (*S*)-**8** resides deeper in the KAc-binding pocket than **3** (Figure 4A). The phenyl ring of (*S*)-**8** occupies the WPF shelf and binds in a similar region as the chlorophenyl moiety of **1** (Figure 4B). It is

possible that substituents on the phenyl ring will be better tolerated in a phenol-derived series than in the ethoxy series described above. We have not investigated this point, but this strategy might lead to compounds with further enhanced

affinity for BRD4(1). Overlaying the X-ray crystal structures of (R)- and (S)-**8** explains the similar affinity of these two compounds for BRD4(1). As the phenyl group binds in the WPF shelf and the 3,5-dimethylisoxazole occupies the KAc-binding pocket, the secondary hydroxyl group is solvent exposed (Figure 4C). Consequently, the configuration at the stereogenic center does not impact the affinity of the compounds for BRD4(1). However, given the reduction in affinity of **17**, compared to **8**, it seems that a tetrahedral atom linking the two aryl rings is favored for BRD4(1) binding. Both enantiomers of compound **8** are observed to form a hydrogen bond between the phenol hydroxyl group and one of the conserved ZA-channel water molecules (Figure 4D); a similar interaction is formed by the quinoline nitrogen atom of compound **5**.[25] As we have discussed previously,[16] it seems that this water molecule is tightly bound to BRD4(1) and hence cannot be displaced easily. It does seem, however, that forming a hydrogen bond with this water molecule might enhance the affinity of **8** for BRD4(1). A combination of this hydrogen bond and binding of the phenyl group in the WPF shelf likely pushes the 3,5-dimethylisoxazole group further into the KAc-binding pocket.

By use of the X-ray crystal structure of (S)-**8** bound to BRD4(1), docking studies (AutoDock Vina) were performed to rationalize the high affinity of **9** for BRD4(1). These studies indicate that it is feasible for **9** to bind to BRD4(1) in an orientation similar to that adopted by **8** (Figure 4E). The 3,5-dimethylisoxazole can occupy the KAc-binding pocket, and the phenyl ring can reside on the WPF shelf. The phenolic oxygen atom of **9** is predicted to form a hydrogen bond with one of the conserved ZA channel water molecules (Figure 4F). The acetate carbonyl group is predicted to form a hydrogen bond with side chain of Q85 and might also interact with the lower ZA channel water molecule. The methyl of the acetate group is predicted to be located in a hydrophobic region close to W81, explaining how the extra steric bulk associated with the acetate moiety might be accommodated. Consequently, the docking studies provide a possible model for the binding of **9** to BRD4(1). It is noted that compound **9** is both an active BRD4(1) ligand and a possible precursor to compound **8** in a cellular setting.

The ALPHA assay was also used to determine the selectivity of **8**, **9**, and **17**, **21−23** for BRD4(1) over the bromodomain of CREBBP (Table 2). Comparison of IC_{50} values indicates that (S)-**8** is 2- to 3-fold selective while compound **9** shows ~7-fold selectivity. The selectivity of **8** was further evaluated across a phylogenetically diverse range of bromodomains (Figure 5). The ALPHA assay indicated that compound **8** displayed less than 25% inhibition of bromodomains contained in this panel at 25 μM (Figure 5), with the exception of BRD4(1) and CREBBP.

BET bromodomain inhibitors have previously shown antiproliferative effects in a variety of hematopoietic malignancies, including AML[25,35,36] and multiple myeloma.[36,37] Consequently, we investigated the effects of compounds **8**, **9**, and **15** in the AML cell line MV4;11, which harbors an MLL−AF4 gene fusion (Table 4).[25] Compounds **8** and **9** had IC_{50} values of 794 and 616 nM, respectively, in an MTS cytotoxicity assay (Supporting Information Figure S4). The weaker BRD4 inhibitor **15**, which has an IC_{50} of approximately 7 times that of **8** and **9** in the BRD4(1) ALPHA assay, was 5-fold less active than **9** in this cytotoxicity assay. Gratifyingly, **8** and **9** showed no appreciable cytotoxicity (>100 μM) in HeLa or U2OS cells
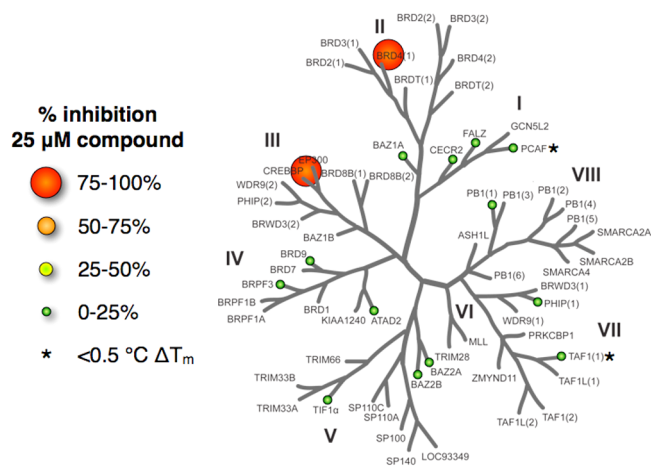

Figure 5. Selectivity of **8** displayed on a phylogenetic tree of bromodomains. Compound **8** showed ~100% inhibition of the BRD4(1) and CREBBP bromodomains at 25 μM. Comparison of IC_{50} values from the ALPHA assays indicates that (S)-**8** is ~3-fold selective for the bromodomain of BRD4(1) over the bromodomain of CREBBP. Investigation of percentage inhibition of the bromodomains from ATAD2, BAZ1A, BAZ2A, BAZ2B, BRD9, BRPF3, CECR2, GCN5L2, PHIP(1), PB1(1), and TIF1α at 25 μM indicated that compound **8** shows little affinity for these bromodomains. In addition, thermal shift analysis of **8** against the bromodomains from PCAF and TAF(1) showed a ΔT_m of less than 0.5 °C, which corresponds to very low affinity for these proteins.

Table 4. Effect of 8, 9, and 15 in Cancer Cell Lines[a]

	IC_{50} (μM)			
cell line	**8**	**9**	**15**	(+)-JQ1 (**1**)
MV4;11 (AML)	0.794	0.616	2.9	0.242
A549 (lung adenocarcinoma)	>10	>10		
H1975 (lung adenocarcinoma)	>10	>10		
U2OS (osteosarcoma)	>100	>100		>100
HeLa (cervical adenocarcinoma)	>100	>100		>100

[a]For MV4;11, A549, and H1975 cells, viability was assessed after a 72 h incubation using MTS. For U2OS and HeLa cells, viability was assessed after a 24 h incubation using WST-1. Further details are provided in the Supporting Information.

over a period of 24 h suggesting that the effects seen in the MV4;11 cells result predominantly from inhibition of the BET BCPs. Over a period of 72 h, compounds **8** and **9** showed less toxicity than (+)-JQ1 in the HeLa and U2OS cells (see Supporting Information Table S2).

We also investigated the effects of **8** and **9** in two lung adenocarcinoma cell lines, A549 and H1975. Compounds **8** and **9** markedly reduced the viability of both cell lines at 100 μM, as determined by an MTS cytotoxicity assay (Supporting Information Figure S4). H1975 appeared to be somewhat more sensitive to these compounds, a finding confirmed by a clonogenic survival assay (Supporting Information Figure S5). The modest effect of **8** and **9** in these cell lines is consistent with the findings of Mertz et al., who observed only weak growth inhibition by BET inhibitor I-BET151 in several solid tumor lines.[36]

Overall, these results suggest that compounds **8** and **9** are cell-permeable compounds without appreciable nonspecific cytotoxicity. These compounds show antiproliferative effects in a leukemic cell line with known sensitivity to BET inhibitors.[25,35,36]

CONCLUSION

We have described the structure-guided optimization of compound **3** to give potent inhibitors of the BET bromodomains (**8** and **9**). The X-ray crystal structures obtained in this work help to demonstrate many of the structural characteristics required for a compound to show high affinity for the BET bromodomains. These compounds show some selectivity over the CREBBP bromodomain and excellent selectivity over other phylogenetically diverse bromodomain classes. On the basis of our structural and docking studies, it seems that constraining the acetate substituent of compound **9** into a five- or six-membered ring might lead to a stronger hydrogen bond with Q85 and provide entropic gains in binding affinity. A re-evaluation of the WPF-shelf-binding ring substituents might also lead to enhanced BRD4(1) affinity and potentially improved selectivity for the BET bromodomains over the CREBBP bromodomain. Assessment of compounds **8** and **9** in a range of cells lines reveals that the compounds have submicromolar IC_{50} values in MV4;11 cells and that the effects are predominantly due to inhibition of the BET BCPs. These compounds will likely prove to be useful tools in the study of the BET bromodomains and are highly ligand-efficient lead compounds for further development.

EXPERIMENTAL SECTION

General Experimental. ^{1}H NMR spectra were recorded on Bruker DPX400 (400 MHz) or Bruker AVII 500 (500 MHz) using deuterochloroform (unless indicated otherwise) as a reference for the internal deuterium lock. The chemical shift data for each signal are given as δ_H in units of parts per million (ppm) relative to tetramethylsilane (TMS) where δ_H(TMS) = 0.00 ppm. The multiplicity of each signal is indicated by s (singlet), br s (broad singlet), d (doublet), t (triplet), q (quartet), dd (doublet of doublets), ddd (doublet of doublet of doublets), or m (multiplet). The number of protons (n) for a given resonance signal is indicated by nH. Coupling constants (J) are quoted in Hz and are recorded to the nearest 0.1 Hz. Identical proton coupling constants (J) are averaged in each spectrum and reported to the nearest 0.1 Hz. The coupling constants are determined by analysis using Bruker TopSpin software.

^{13}C NMR spectra were recorded on a Bruker AVII 500 (126 MHz) spectrometer with broadband proton decoupling and internal deuterium lock. The chemical shift data for each signal are given as δ_C in units of parts per million (ppm) relative to tetramethylsilane (TMS) where δ_C(TMS) = 0.00 ppm.

^{19}F NMR spectra were recorded on a Bruker AVII 500 (470 MHz) using a broadband proton decoupling pulse sequence and deuterium internal lock. The chemical shift data for each signal are given as δ_F in units of parts per million (ppm).

Mass spectra were acquired on either a Micromass LCT Premier spectrometer (low resolution) or a Bruker MicroTOF spectrometer (high resolution), operating in positive or negative mode, from solutions of MeOH. m/z values are reported in daltons and followed by their percentage abundance in parentheses.

Melting points were determined using a Leica Galen III hot stage microscope and are uncorrected.

Compound purity for all tested compounds was determined by elemental analysis, obtained at the Elemental Analysis Service, London Metropolitan University, London. Elemental analysis was carried out in duplicate; average values are reported in Supporting Information. For all tested compounds, experimentally determined hydrogen, carbon, and nitrogen composition was within ±0.4% of the expected value, implying a purity of >95%.

General Procedure for Grignard Reaction of Aryl Bromide and 11. To a dry two-necked flask, equipped with a condenser, containing Mg turnings (66 mg, 2.45 mmol, 3.0 equiv) and a crystal of iodine was added dry Et_2O or dry THF (20 mL, as stated) under a nitrogen atmosphere. Aryl bromide (2.69 mmol, 3.3 equiv) was then added either neat if a liquid or as a solution in THF (269 mM, 10 mL). The mixture was heated gently to initiate Grignard reagent formation, then heated under reflux until all the Mg had reacted. The mixture was then cooled to 0 °C and added slowly to a solution of **11** (200 mg, 815 μmol, 1.0 equiv) in Et_2O or THF (81.5 mM, 10 mL, as stated) at 0 °C under a nitrogen atmosphere. The solution was warmed to room temperature. On consumption of aldehyde (as indicated by TLC), the reaction was quenched with H_2O and HCl (1 M aqueous). The phases were separated, and the aqueous layer was extracted with Et_2O. The combined organic layers were washed with H_2O and brine, dried ($MgSO_4$), filtered, and concentrated in vacuo. The crude residues were purified by silica gel chromatography (gradient elution, Et_2O/ petroleum ether).

Synthetic Procedure and Characterization of Compounds 8, 9, 12−16, 21−23. *(3-(3,5-Dimethylisoxazol-4-yl)-5-ethoxyphenyl)- (phenyl)methanol 12.* To a solution of **11** (79 mg, 322 μmol, 1.0 equiv) in dry THF (5 mL) under a nitrogen atmosphere was added PhMgBr (0.9 M in THF, 716 μL, 644 μmol, 2.0 equiv) dropwise at 0 °C. The solution was warmed to room temperature over 17 h, then quenched with HCl (1 M aqueous, 10 mL) and extracted with Et_2O (3 × 10 mL). The combined organic layers were washed with H_2O (2 × 30 mL) and brine (30 mL), dried ($MgSO_4$), filtered, and concentrated in vacuo. Purification by silica gel column chromatography (gradient elution, 10% → 60% Et_2O/petroleum ether) gave **12** as a colorless oil (83 mg, 80%). ^{1}H NMR (500 MHz, $CDCl_3$) 1.42 (3H, t, J = 7.0 Hz), 2.23 (3H, s), 2.29 (1H, d, J = 3.3 Hz), 2.37 (3H, s), 4.04 (2H, q, J = 7.0 Hz), 5.85 (1H, d, J = 3.3 Hz), 6.67 (1H, dd, J = 2.2, 1.6 Hz), 6.82 (1H, s), 6.96 (1H, dd, J = 2.2, 1.1 Hz), 7.29 (1H, tt, J = 7.2, 1.5 Hz), 7.34−7.43 (4H, m); HRMS m/z (ES[+]) found [M + Na][+] 346.1406; $C_{20}H_{21}NNaO_3$ requires M[+] 346.1414; m/z (ES[+]) 324 ([M + H][+], 24), 346 ([M + Na][+], 33), 669 ([2M + Na][+], 100).

(3-(3,5-Dimethylisoxazol-4-yl)-5-ethoxyphenyl)(4-fluorophenyl)- methanol 13. Following the general procedure, 1-bromo-4-fluorobenzene (471 mg, 296 μL) and Mg turnings in THF were heated under reflux for 3 h. Following addition of the resultant cloudy yellow suspension to **11** in THF, the mixture was stirred for 4.5 h. Then the reaction was quenched with H_2O (15 mL) and HCl (1 M aqueous, 15 mL). The phases were separated, and the aqueous layer was extracted with Et_2O (3 × 30 mL). The combined organic layers were washed with H_2O (90 mL) and brine (90 mL), dried ($MgSO_4$), filtered, and concentrated in vacuo. Purification by silica gel column chromatography (gradient elution, 20% → 80% Et_2O/petroleum ether) gave **13** as a pale yellow viscous gum (170 mg, 61%). ^{1}H NMR (500 MHz, $CDCl_3$) 1.41 (3H, t, J = 7.0 Hz), 2.19 (3H, s), 2.35 (3H, s), 2.98 (1H, br s), 4.03 (2H, q, J = 7.0 Hz), 5.80 (1H, s), 6.66 (1H, dd, J = 2.3, 1.5 Hz), 6.79 (1H, s), 6.92 (1H, s), 6.98−7.05 (2H, m), 7.32−7.38 (2H, m); HRMS m/z (ES[+]) found 364.1318; $C_{20}H_{20}FNNaO_3$ requires M[+] 364.1319; m/z (ES[+]) 342 ([M + H][+], 12), 364 ([M + Na][+], 19), 396 ([M + Na + MeOH][+], 8), 705 ([2M + Na][+], 100).

(3-(3,5-Dimethylisoxazol-4-yl)-5-ethoxyphenyl)(3-fluorophenyl)- methanol 14. Following the general procedure, 1-bromo-3-fluorobenzene (471 mg, 300 μL) and Mg turnings in Et_2O were heated under reflux for 2 h. Following addition of the resultant cloudy yellow suspension to **11** in Et_2O, the mixture was stirred for 2 h. Then the reaction was quenched with H_2O (10 mL) and HCl (1 M aqueous, 10 mL). The phases were separated, and the aqueous layer was extracted with Et_2O (2 × 20 mL). The combined organic layers were washed with H_2O (60 mL) and brine (60 mL), dried ($MgSO_4$), filtered, and concentrated in vacuo. Purification by silica gel column chromatography (gradient elution, 20% → 80% Et_2O/petroleum ether) gave **14** as a pale yellow viscous gum (255 mg, 92%). ^{1}H NMR (500 MHz, $CDCl_3$) 1.42 (3H, t, J = 7.0 Hz), 2.21 (3H, s), 2.36 (3H, s), 2.87 (1H, d, J = 3.4 Hz), 4.03 (2H, q, J = 7.0 Hz), 5.81 (1H, d, J = 3.4 Hz), 6.68 (1H, dd, J = 2.1, 1.3 Hz), 6.80 (1H, dd, J = 1.4, 1.3 Hz), 6.92 (1H, dd, J = 2.1, 1.4 Hz), 6.93−6.99 (1H, m), 7.10−7.14 (1H, m), 7.14−7.19 (1H, m), 7.27−7.33 (1H, m); HRMS m/z (ES[+]) found 364.1312; $C_{20}H_{20}FNNaO_3$ requires M[+] 364.1319; m/z (ES[+]) 342 ([M + H][+], 4), 364 ([M + Na][+], 14), 396 ([M + Na + MeOH][+], 10), 705 ([2M + Na][+], 100).

(4-Chlorophenyl)(3-(3,5-dimethylisoxazol-4-yl)-5-ethoxyphenyl)-methanol 15. Following the general procedure, 1-bromo-4-chlorobenzene (515 mg) and Mg turnings in THF were heated under reflux for 2.5 h. Following addition of the resultant cloudy yellow suspension to **11** in THF, the mixture was stirred for 3 h. Then the reaction was quenched with H_2O (10 mL) and HCl (1 M aqueous, 20 mL). The phases were separated, and the aqueous layer was extracted with Et_2O (3 × 40 mL). The combined organic layers were washed with H_2O (120 mL) and brine (120 mL), dried ($MgSO_4$), filtered, and concentrated in vacuo. Purification by silica gel column chromatography (gradient elution, 20% → 80% Et_2O/petroleum ether) gave **15** as a colorless viscous gum that slowly crystallized to a colorless solid under vacuum (195 mg, 67%). Mp 103−104 °C; ^{1}H NMR (500 MHz, CDCl$_3$) 1.42 (3H, t, J = 7.0 Hz), 2.22 (3H, s), 2.37 (3H, s), 2.60 (1H, br s), 4.03 (2H, q, J = 7.0 Hz), 5.81 (1H, s), 6.68 (1H, s), 6.80 (1H, s), 6.91 (1H, s), 7.29−7.37 (4H, m); HRMS m/z (ES$^+$) found 380.1018, $C_{20}H_{20}ClNNaO_3$ requires M$^+$ 380.1024; m/z (ES$^+$) 358 ([M + H]$^+$, 7), 380 ([M + Na]$^+$, 7), 412 ([M + Na + MeOH]$^+$, 9), 737 ([2M + Na]$^+$, 100).

(3-Chlorophenyl)(3-(3,5-dimethylisoxazol-4-yl)-5-ethoxyphenyl)-methanol 16. Following the general procedure, 1-bromo-3-chlorobenzene (515 mg, 316 μL) and Mg turnings in THF were heated under reflux for 1 h. Following addition of the resultant yellow solution to **11** in THF, the mixture was stirred for 2 h. Then the reaction was quenched with H_2O (10 mL) and HCl (1 M aqueous, 10 mL). The phases were separated, and the aqueous layer was extracted with Et_2O (3 × 40 mL). The combined organic layers were washed with H_2O (120 mL) and brine (120 mL), dried ($MgSO_4$), filtered, and concentrated in vacuo. Purification by silica gel column chromatography (gradient elution, 20% → 80% Et_2O/petroleum ether) gave **16** as a colorless viscous gum (262 mg, 90%). ^{1}H NMR (500 MHz, CDCl$_3$) 1.42 (3H, t, J = 7.0 Hz), 2.20 (3H, s), 2.36 (3H, s), 2.88 (1H, br s), 4.04 (2H, q, J = 7.0 Hz), 5.78 (1H, s), 6.67 (1H, s), 6.79 (1H, s), 6.92 (1H, s), 7.21−7.29 (3H, m), 7.40 (1H, s); HRMS m/z (ES$^+$) found 380.1018, $C_{20}H_{20}ClNNaO_3$ requires M$^+$ 380.1024; m/z (ES$^+$) 380 ([M + Na]$^+$, 4), 737 ([2M + Na]$^+$, 100).

3-(3,5-Dimethylisoxazol-4-yl)-5-(hydroxy(phenyl)methyl)phenol 8. To a solution of **10** (250 mg, 1.02 mmol, 1.0 equiv) in dry THF (20 mL) under a nitrogen atmosphere was added PhMgBr (0.9 M in THF, 3.4 mL, 3.06 mmol, 3.0 equiv) dropwise at 0 °C. The solution was warmed to room temperature over 1 h, then quenched with HCl (1 M aqueous, 10 mL) and concentrated in vacuo to remove THF. The residues were extracted with EtOAc (3 × 20 mL). The combined organic layers were washed with H_2O (2 × 40 mL) and brine (40 mL), dried ($MgSO_4$), filtered, and concentrated in vacuo. Purification by silica gel column chromatography (gradient elution, 10% → 50% EtOAc/petroleum ether) gave **8** as a pale yellow solid (273 mg, 91%). Mp 187−188 °C (CHCl$_3$); ^{1}H NMR (500 MHz, acetone-d_6) 2.21 (3H, s), 2.38 (3H, s), 4.95 (1H, d, J = 3.1 Hz), 5.84 (1H, d, J = 3.1 Hz), 6.71 (1H, dd, J = 2.3, 1.6 Hz), 6.91−6.94 (1H, m), 6.96 (1H, dd, J = 2.3, 1.4 Hz), 7.24 (1H, tt, J = 7.3, 1.3 Hz), 7.31−7.36 (2H, m), 7.46−7.50 (2H, m), 8.50 (1H, s); HRMS m/z (ES$^+$) found 318.1102, $C_{18}H_{17}NNaO_3$ requires M$^+$ 318.1101; m/z (ES$^-$) 294 ([M − H]$^-$, 48), 330 [M + Cl]$^-$, 14), 408 ([M + TFA − H]$^-$, 9), 589 ([2M − H]$^-$, 100), 884 ([3M − H]$^-$, 18).

3-(3,5-Dimethylisoxazol-4-yl)-5-(hydroxy(phenyl)methyl)phenyl Acetate 9. Following the procedure of Srivastava et al.,[38] solid NaOH dissolved in a minimum amount of H_2O (37 mg, 915 μmol, 2.7 equiv) was added to a stirred suspension of **8** (100 mg, 339 μmol, 1.0 equiv) in ^{i}PrOH (5 mL). Ac_2O (93 mg, 86 μL, 915 μmol, 2.7 equiv) was added dropwise, and the solution was stirred at room temperature for 1 h. The solution was then concentrated in vacuo to remove ^{i}PrOH and diluted with 10 mL of H_2O, then extracted with EtOAc (3 × 10 mL). The combined organic layers were washed with H_2O (30 mL) and brine (30 mL), dried ($MgSO_4$), filtered, and concentrated in vacuo. Purification by silica gel column chromatography (gradient elution, 10% → 50% EtOAc/petroleum ether) gave **9** as a colorless oil (104 mg, 90%). ^{1}H NMR (500 MHz, CDCl$_3$) 2.22 (3H, s), 2.30 (3H, s), 2.37 (3H, s), 2.63 (1H, d, J = 2.9 Hz), 5.86 (1H, d, J = 2.9 Hz,), 6.90 (1H, dd, J = 1.7, 1.5 Hz), 7.11 (1H, dd, J = 1.7, 1.5 Hz), 7.15 (1H,

dd, J = 1.7, 1.5 Hz), 7.28−7.32 (1H, m), 7.33−7.42 (4H, m); HRMS m/z (ES$^+$) found 360.1206; $C_{20}H_{19}NNaO_4$ requires M$^+$ 360.1206; m/z (ES$^+$) 338 ([M + H]$^+$, 35), 360 ([M + Na]$^+$, 100), 697 ([2M + Na]$^+$, 95).

(3-(3,5-Dimethylisoxazol-4-yl)-5-hydroxyphenyl)(phenyl)-methanone 17. To a solution of alcohol **8** (207 mg, 701 μmol) in anhydrous 1,4-dioxane (10 mL) was added activated MnO_2 (305 mg, 3.50 mmol, 5 equiv). The mixture was stirred under nitrogen at 80 °C for 15 h, after which time further MnO_2 (152 mg, 1.75 mmol, 2.5 equiv) was added, and stirring was continued at 80 °C for 9 h. Further MnO_2 (152 mg, 1.75 mmol, 2.5 equiv) was then added, and stirring was continued at 80 °C for 29 h. The mixture was cooled to room temperature and filtered through Celite (eluent CH_2Cl_2), then concentrated in vacuo. Purification by silica gel column chromatography (gradient elution, gradient 20% → 50% EtOAc/40−60 °C petroleum ether, then further purification of mixed fractions, 20% → 35% EtOAc/40−60 °C petroleum ether) gave **17** as a cream solid (172 mg, 84%). R_f = 0.43 (50% EtOAc/40−60 °C petroleum ether); mp 188−190 °C (acetone); ^{1}H NMR (500 MHz, acetone-d_6) 2.27 (3H, s), 2.45 (3H, s), 7.13 (1H, dd, J = 2.4, 1.5 Hz), 7.20 (1H, dd, J = 1.5, 1.5 Hz), 7.27 (1H, dd, J = 2.4, 1.5 Hz), 7.55−7.62 (2H, m), 7.66−7.71 (1H, m), 7.82−7.88 (2H, m); HRMS m/z (ES$^+$) found 316.0938; $C_{18}H_{15}NNaO_3$ requires M$^+$ 316.0944; m/z (ES$^-$) 292 ([M − H]$^-$, 100), 328 ([M + Cl]$^-$, 13).

(3-(3,5-Dimethylisoxazol-4-yl)-5-methoxyphenyl)(phenyl)-methanol 21. To a solution of **18** (80 mg, 346 μmol, 1.0 equiv) in dry THF (5 mL) under a nitrogen atmosphere was added PhMgBr (0.9 M in THF, 769 μL, 692 μmol, 2.0 equiv) dropwise at 0 °C. The solution was stirred for 1 h, then quenched with HCl (1 M aqueous, 5 mL) and concentrated in vacuo to remove THF. The residues were extracted with EtOAc (3 × 5 mL). The combined organic layers were washed with H_2O (20 mL) and brine (20 mL), dried ($MgSO_4$), filtered, and concentrated in vacuo. Purification by silica gel column chromatography (gradient elution, 30% → 80% Et_2O petroleum ether) gave **21** as a colorless oil (66 mg, 76%). ^{1}H NMR (500 MHz, CDCl$_3$) 2.21 (3H, s), 2.36 (3H, s), 2.68 (1H, s), 3.82 (3H, s), 5.84 (1H, s), 6.68 (1H, dd, J = 2.3, 1.3 Hz), 6.83 (1H, dd, J = 1.3, 1.3 Hz), 6.98 (1H, dd, J = 2.3, 1.3 Hz), 7.26−7.31 (1H, m), 7.33−7.38 (2H, m), 7.38−7.42 (2H, m); HRMS m/z (ES$^+$) found [M + Na]$^+$ 332.1257; $C_{19}H_{19}NNaO_3$ requires M$^+$ 332.1257; m/z (ES$^+$) 332 ([M + Na]$^+$, 12), 364 ([M + Na + MeOH]$^+$, 6), 641 ([2M + Na]$^+$, 100).

(3-(3,5-Dimethylisoxazol-4-yl)-5-(2-methoxyethoxy)phenyl)-(phenyl)methanol 22. To a solution of **19** (150 mg, 545 μmol, 1.0 equiv) in anhydrous THF (10 mL) under a nitrogen atmosphere was added PhMgBr (0.9 M in THF, 1.2 mL, 1.08 mmol, 2.0 equiv) dropwise at 0 °C. The solution was warmed to room temperature and stirred for 90 min, then quenched with HCl (1 M aqueous, 5 mL) and concentrated in vacuo to remove THF. The residues were extracted with EtOAc (3 × 5 mL). The combined organic layers were washed with H_2O (15 mL) and brine (15 mL), dried ($MgSO_4$), filtered, and concentrated in vacuo. Purification by silica gel column chromatography (gradient elution, 6% → 60% EtOAc/petroleum ether) gave **22** as a colorless oil that crystallized slowly under vacuum to give a colorless solid (159 mg, 83%). Mp 70−73 °C; ^{1}H NMR (500 MHz, CDCl$_3$) 2.20 (3H, s), 2.35 (3H, s), 2.74 (1H, d, J = 3.2 Hz), 3.44 (3H, s), 3.74 (2H, t, J = 4.6 Hz), 4.11 (2H, t, J = 4.6 Hz), 5.82 (1H, d, J = 3.2 Hz), 6.71 (1H, dd, J = 1.9, 1.5 Hz), 6.83 (1H, dd, J = 1.6, 1.5 Hz), 6.98 (1H, dd, J = 1.9, 1.6 Hz), 7.25−7.30 (1H, m), 7.31−7.40 (4H, m); HRMS m/z (ES$^+$) found [M + Na]$^+$ 376.1515; $C_{21}H_{23}NNaO_4$ requires M$^+$ 376.1519; m/z (ES$^+$) 376 ([M + Na]$^+$, 23), 729 ([2M + Na]$^+$, 100).

2-(3-(3,5-Dimethylisoxazol-4-yl)-5-(hydroxy(phenyl)methyl)-phenoxy)ethanol 23. To a solution of **20** (125 mg, 478 μmol, 1.0 equiv) in anhydrous THF (8 mL) under a nitrogen atmosphere was added PhMgBr (0.9 M in THF, 1.6 mL, 1.44 mmol, 3.0 equiv) dropwise at 0 °C. The solution was warmed to room temperature and stirred for 3 h, then quenched with aqueous HCl (1 M, 10 mL) and concentrated in vacuo to remove THF. The residues were extracted with EtOAc (3 × 10 mL). The combined organic layers were washed with H_2O (20 mL) and brine (20 mL), dried ($MgSO_4$), filtered, and

concentrated in vacuo. The residues were purified by silica gel column chromatography (gradient elution, 40% → 80% EtOAc/petroleum ether) to give a colorless gum that crystallized slowly under vacuum to give a colorless solid. Repeated recrystallization from boiling $CHCl_3$/cyclohexane (1:1) gave **23** as a colorless solid (100 mg, 62%). Mp 133−134 °C (1:1 $CHCl_3$/cyclohexane); ^1H NMR (500 MHz, DMSO-d_6) 2.20 (3H, s), 2.38 (3H, s), 3.71 (2H, dt, J = 5.5, 5.0 Hz), 4.00 (2H, t, J = 5.0 Hz), 4.86 (1H, t, J = 5.5 Hz), 5.73 (1H, d, J = 3.9 Hz), 5.96 (1H, d, J = 3.9 Hz), 6.76 (1H, dd, J = 2.2, 1.4 Hz), 6.93−6.96 (1H, m), 6.96−6.98 (1H, m), 7.21 (1H, t, J = 7.5 Hz), 7.31 (2H, dd, J = 7.5, 7.5 Hz), 7.43 (2H, d, J = 7.5, Hz); HRMS m/z (ES$^+$) found [M + Na]$^+$ 362.1353; $C_{20}H_{21}NNaO_4$ requires M$^+$ 362.1363; m/z (ES$^+$) 362 ([M + Na]$^+$, 7), 701 ([2M + Na]$^+$, 100).

Docking Studies. *Preparation of the Receptor.* The receptor was initially prepared by adding polar hydrogen atoms at pH 7.4 using Protonate3D in MOE. Gasteiger charges were then assigned using AutoDock's graphical user interface AutoDockTools (ADT, version 1.5.4). Following the addition of Gasteiger charges, ADT was implemented to build a "united atom model" of the receptor by merging nonpolar hydrogen atoms and adding their partial charges to their parent carbon atoms.

Preparation of the Ligands. The ligands were prepared by adding polar hydrogens atoms at pH 7.4 using Protonate3D in Molecular Operating Environment (MOE), version 2011.10. MOE then assigned Gasteiger charges before performing an energy minimization using an MMFF94x force field with a 0.05 gradient. AutoDock's graphical user interface AutoDockTools (ADT, version 1.5.4) was subsequently used to build a "united atom model" of the ligands by merging nonpolar hydrogens and adding their partial charges to their parent carbon atoms.

Individual Docking with AutoDock Vina (Version 1.1.2). The search space was defined as a cubic box with dimensions 18 Å × 18 Å × 18 Å and center x = 30.048, y = 16.281, z = −1.723. The exhaustiveness and number of modes were both set to 20, and all other parameters were kept at their default values.

Biological Evaluation. *Protein Expression and Purification.* Proteins were cloned, expressed, and purified as previously described.[17]

Peptides. H4Ac4 peptide (BRD4 assay, H_2N-SGRGK(Ac)GGK-(Ac)GLGK(Ac)GGAK(Ac)RHRK(biotin)-COOH) and H3K56Ac peptide (CREBBP assay, H_2N-ALREIRRYQK(Ac)STELLIRKLK-(biotin)-COOH) were synthesized by Tufts University Core Facility.

AlphaScreen Peptide Displacement Assay (ALPHA Assay). Bromodomain AlphaScreen assays were carried out as previously described.[24,30] All experiments were carried out in duplicate on the same plate.

Cytotoxicity Assay. Viability of MV4;11, H549, and H1975 cells was monitored by MTS-based CellTiter 96 AQueous nonradioactive cell proliferation assay (Promega, Madison, WI). Viability of U2OS and HeLa cells was monitored by WST-based cell proliferation kit (Roche, Mannheim, Germany). Further details are provided in Supporting Information

ASSOCIATED CONTENT

Ⓢ Supporting Information

Enantiomeric purity determination of **8** by chiral HPLC, stability of (+)-**8** in aqueous buffer, SPR steady state affinity analysis of (R)- and (S)-**8** binding to BRD4(1), comparison of the BRD4(1) and CREBBP bromodomains, BRD4(1) and CREBBP bromodomain sequence alignment, MTS viability assays for MV4;11, A549, and H1975 cells, steady state analysis parameters for (R)- and (S)-**8** binding to BRD4(1), crystallographic information, further general experimental details, synthesis and characterization of compounds **10**, **11**, **18−20**, and further characterization (^{13}C and ^{19}F NMR, elemental analysis) for compounds **8**, **9**, **12−17**, **21−23**. This material is available free of charge via the Internet at http://pubs.acs.org.

Accession Codes

Atomic coordinates and structure factors for the reported crystal structures have been deposited with the Protein Data Bank under accession codes 4J0R [(R)-**8**] and 4J0S [(S)-**8**].

AUTHOR INFORMATION

Corresponding Author

*Telephone: +44 (0)1865 285 109. Fax: +44 (0)1865 285 002. E-mail: stuart.conway@chem.ox.ac.uk.

Author Contributions

The manuscript was written with contributions of all authors. All authors have given approval to the final version of the manuscript.

Notes

The authors declare no competing financial interest.

ABBREVIATIONS USED

ALPHA, amplified luminescent proximity homogeneous assay; AML, acute myeloid leukemia; BET, bromodomain and extra terminal domain; BCP, bromodomain-containing protein; BRD2(1)/(2), first/second bromodomain of BRD2; BRD4-(1)/(2), first/second bromodomain of BRD4; BRDT, bromodomain, testis-specific; CREB, cAMP response element-binding protein; CREBBP, CREB binding protein; HAT, histone acetyltransferase; HDAC, histone deacetylase; KAc, acetyllysine; MLL, mixed lineage leukemia; MTS, (3-(4,5-dimethylthiazol-2-yl)-5-(3-carboxymethoxyphenyl)-2-(4-sulfophenyl)-2H-tetrazolium); PTM, post-translational modification; WST-1, water-soluble tetrazolium 1

REFERENCES

(1) Allfrey, V.; Faulkner, R.; Mirsky, A. Acetylation and methylation of histones and their possible role in regulation of RNA synthesis. *Proc. Natl. Acad. Sci. U.S.A.* **1964**, *51*, 786−794.

(2) Kouzarides, T. Acetylation: a regulatory modification to rival phosphorylation? *EMBO J.* **2000**, *19*, 1176−1179.

(3) Arrowsmith, C. H.; Bountra, C.; Fish, P. V.; Lee, K.; Schapira, M. Epigenetic protein families: a new frontier for drug discovery. *Nat. Rev. Drug Discovery* **2012**, *11*, 384−400.

(4) Strahl, B. D.; Allis, C. D. The language of covalent histone modifications. *Nature* **2000**, *403*, 41−45.

(5) Gardner, K. E.; Allis, C. D.; Strahl, B. D. Operating on chromatin, a colorful language where context matters. *J. Mol. Biol.* **2011**, *409*, 36−46.

(6) Conway, S. J. Bromodomains: Are readers right for epigenetic therapy? *ACS Med. Chem. Lett.* **2012**, *3*, 691−694.

(7) Dhanak, D. Cracking the code: the promise of epigenetics. *ACS Med. Chem. Lett.* **2012**, *3*, 521−523.

(8) Zeng, L.; Zhou, M. Bromodomain: an acetyl-lysine binding domain. *FEBS Lett.* **2002**, *513*, 124−128.

(9) Filippakopoulos, P.; Knapp, S. The bromodomain interaction module. *FEBS Lett.* **2012**, *586*, 2692−2704.

(10) Filippakopoulos, P.; Picaud, S.; Mangos, M.; Keates, T.; Lambert, J.-P.; Barsyte-Lovejoy, D.; Felletar, I.; Volkmer, R.; Muller, S.; Pawson, T.; Gingras, A.-C.; Arrowsmith, C. H.; Knapp, S. Histone recognition and large-scale structural analysis of the human bromodomain family. *Cell* **2012**, *149*, 214−231.

(11) Muller, S.; Filippakopoulos, P.; Knapp, S. Bromodomains as therapeutic targets. *Expert Rev. Mol. Med.* **2011**, *13*, e29.

(12) Prinjha, R. K.; Witherington, J.; Lee, K. Place your BETs: the therapeutic potential of bromodomains. *Trends Pharmacol. Sci.* **2012**, *33*, 146−153.

(13) Chung, C.-W.; Tough, D. F. Bromodomains: a new target class for small molecule drug discovery. *Drug Discovery Today: Ther. Strategies* **2012**, *9*, e111−e120.

(14) Chung, C.-W. Small molecule bromodomain inhibitors: extending the druggable genome. *Prog. Med. Chem.* **2012**, *51*, 1−55.

(15) Brennan, P.; Filippakopoulos, P.; Knapp, S. The therapeutic potential of acetyl-lysine and methyl-lysine effector domains. *Drug Discovery Today: Ther. Strategies* **2012**, *9*, e101−e110.

(16) Hewings, D. S.; Rooney, T. P. C.; Jennings, L. E.; Hay, D. A.; Schofield, C. J.; Brennan, P. E.; Knapp, S.; Conway, S. J. Progress in the development and application of small molecule inhibitors of bromodomain-acetyl-lysine interactions. *J. Med. Chem.* **2012**, *55*, 9393−9413.

(17) Filippakopoulos, P.; Qi, J.; Picaud, S.; Shen, Y.; Smith, W. B.; Fedorov, O.; Morse, E. M.; Keates, T.; Hickman, T. T.; Felletar, I.; Philpott, M.; Munro, S.; McKeown, M. R.; Wang, Y.; Christie, A. L.; West, N.; Cameron, M. J.; Schwartz, B.; Heightman, T. D.; La Thangue, N.; French, C. A.; Wiest, O.; Kung, A. L.; Knapp, S.; Bradner, J. E. Selective inhibition of BET bromodomains. *Nature* **2010**, *468*, 1067−1073.

(18) Nicodeme, E.; Jeffrey, K. L.; Schaefer, U.; Beinke, S.; Dewell, S.; Chung, C.-W.; Chandwani, R.; Marazzi, I.; Wilson, P.; Coste, H.; White, J.; Kirilovsky, J.; Rice, C. M.; Lora, J. M.; Prinjha, R. K.; Lee, K.; Tarakhovsky, A. Suppression of inflammation by a synthetic histone mimic. *Nature* **2010**, *468*, 1119−1123.

(19) Adachi, K.; Hikawa, H.; Hamada, M.; Endoch, J.-I.; Ishibichi, S.; Fujie, N.; Tanaka, M.; Sugahara, K.; Oshita, K.; Murata, M. Thienotriazolodiazepine Compound and a Medicinal Use Thereof. PCT/JP2006/310709 (WO/2006/129623), 2006.

(20) Miyoshi, S.; Ooike, S.; Iwata, K.; Hikawa, H.; Sugahara, K. Antitumor Agent. PCT/JP2008/073864 (WO/2009/084693), 2009.

(21) Chung, C.-W.; Coste, H.; White, J. H.; Mirguet, O.; Wilde, J.; Gosmini, R. L.; Delves, C.; Magny, S. M.; Woodward, R.; Hughes, S. A.; Boursier, E. V.; Flynn, H.; Bouillot, A. M.; Bamborough, P.; Brusq, J.-M. G.; Gellibert, F. J.; Jones, E. J.; Riou, A. M.; Homes, P.; Martin, S. L.; Uings, I. J.; Toum, J.; Clément, C. A.; Boullay, A.-B.; Grimley, R. L.; Blandel, F. M.; Prinjha, R. K.; Lee, K.; Kirilovsky, J.; Nicodeme, E. Discovery and characterization of small molecule inhibitors of the BET family bromodomains. *J. Med. Chem.* **2011**, *54*, 3827−3838.

(22) Filippakopoulos, P.; Picaud, S.; Fedorov, O.; Keller, M.; Wrobel, M.; Morgenstern, O.; Bracher, F.; Knapp, S. Benzodiazepines and benzotriazepines as protein interaction inhibitors targeting bromodomains of the BET family. *Bioorg. Med. Chem.* **2012**, *20*, 1878−1886.

(23) Zhang, G.; Liu, R.; Zhong, Y.; Plotnikov, A. N.; Zhang, W.; Zeng, L.; Rusinova, E.; Gerona-Nevarro, G.; Moshkina, N.; Joshua, J.; Chuang, P. Y.; Ohlmeyer, M.; He, J. C.; Zhou, M.-M. Down-regulation of NF-κB transcriptional activity in HIV-associated kidney disease by BRD4 inhibition. *J. Biol. Chem.* **2012**, *287*, 28840−28851.

(24) Hewings, D. S.; Wang, M.; Philpott, M.; Fedorov, O.; Uttarkar, S.; Filippakopoulos, P.; Picaud, S.; Vuppusetty, C.; Marsden, B.; Knapp, S.; Conway, S. J.; Heightman, T. D. 3,5-Dimethylisoxazoles act as acetyl-lysine-mimetic bromodomain ligands. *J. Med. Chem.* **2011**, *54*, 6761−6770.

(25) Dawson, M. A.; Prinjha, R. K.; Dittmann, A.; Giotopoulos, G.; Bantscheff, M.; Chan, W.-I.; Robson, S. C.; Chung, C.-W.; Hopf, C.; Savitski, M. M.; Huthmacher, C.; Gudgin, E.; Lugo, D.; Beinke, S.; Chapman, T. D.; Roberts, E. J.; Soden, P. E.; Auger, K. R.; Mirguet, O.; Doehner, K.; Delwel, R.; Burnett, A. K.; Jeffrey, P.; Drewes, G.; Lee, K.; Huntly, B. J. P.; Kouzarides, T. Inhibition of BET recruitment to chromatin as an effective treatment for MLL-fusion leukaemia. *Nature* **2011**, *478*, 529−533.

(26) Hay, D.; Fedorov, O.; Filippakopoulos, P.; Martin, S.; Philpott, M.; Picaud, S.; Hewings, D. S.; Uttakar, S.; Heightman, T. D.; Conway, S. J.; Knapp, S.; Brennan, P. E. The design and synthesis of 5 and 6-isoxazolylbenzimidazoles as selective inhibitors of the BET bromodomains. *Med. Chem. Commun.* **2013**, *4*, 140−144.

(27) Fish, P. V.; Filippakopoulos, P.; Bish, G.; Brennan, P. E.; Bunnage, M. E.; Cook, A. S.; Federov, O.; Gerstenberger, B. S.; Jones, H.; Knapp, S.; Marsden, B.; Nocka, K.; Owen, D. R.; Philpott, M.; Picaud, S.; Primiano, M. J.; Ralph, M. J.; Sciammetta, N.; Trzupek, J. D. Identification of a chemical probe for bromo and extra C-terminal bromodomain inhibition through optimization of a fragment-derived hit. *J. Med. Chem.* **2012**, *55*, 9831−9837.

(28) Chung, C.-W.; Dean, A. W.; Woolven, J. M.; Bamborough, P. Fragment-based discovery of bromodomain inhibitors part 1: inhibitor binding modes and implications for lead discovery. *J. Med. Chem.* **2012**, *55*, 576−586.

(29) Bamborough, P.; Diallo, H.; Goodacre, J. D.; Gordon, L.; Lewis, A.; Seal, J. T.; Wilson, D. M.; Woodrow, M. D.; Chung, C.-W. Fragment-based discovery of bromodomain inhibitors part 2: optimization of phenylisoxazole sulfonamides. *J. Med. Chem.* **2012**, *55*, 587−596.

(30) Philpott, M.; Yang, J.; Tumber, T.; Fedorov, O.; Uttarkar, S.; Filippakopoulos, P.; Picaud, S.; Keates, T.; Felletar, I.; Ciulli, A.; Knapp, S.; Heightman, T. D. Bromodomain-peptide displacement assays for interactome mapping and inhibitor discovery. *Mol. BioSyst.* **2011**, *7*, 2899−2908.

(31) Dunitz, J. D. The entropic cost of bound water in crystals and biomolecules. *Science* **1994**, *264*, 670.

(32) Ellermann, M.; Jakob-Roetne, R.; Lerner, C.; Borroni, E.; Schlatter, D.; Roth, D.; Ehler, A.; Rudolph, M. G.; Diederich, F. Molecular recognition at the active site of catechol-*o*-methyltransferase: energetically favorable replacement of a water molecule imported by a bisubstrate inhibitor. *Angew. Chem., Int. Ed.* **2009**, *48*, 9092−9096.

(33) Kohler, P. C.; Ritschel, T.; Schweizer, W. B.; Klebe, G.; Diederich, F. High-affinity inhibitors of tRNA-guanine transglycosylase replacing the function of a structural water cluster. *Chem.—Eur. J.* **2009**, *15*, 10809−10817.

(34) Salonen, L. M.; Holland, M. C.; Kaib, P. S. J.; Haap, W.; Benz, J.; Mary, J.-L.; Kuster, O.; Schweizer, W. B.; Banner, D. W.; Diederich, F. Molecular recognition at the active site of factor Xa: cation−π interactions, stacking on planar peptide surfaces, and replacement of structural water. *Chem.—Eur. J.* **2012**, *18*, 213−222.

(35) Zuber, J.; Shi, J.; Wang, E.; Rappaport, A. R.; Herrmann, H.; Sison, E. A.; Magoon, D.; Qi, J.; Blatt, K.; Wunderlich, M.; Taylor, M. J.; Johns, C.; Chicas, A.; Mulloy, J. C.; Kogan, S. C.; Brown, P.; Valent, P.; Bradner, J. E.; Lowe, S. W.; Vakoc, C. R. RNAi screen identifies Brd4 as a therapeutic target in acute myeloid leukaemia. *Nature* **2011**, *478*, 524−528.

(36) Mertz, J. A.; Conery, A. R.; Bryant, B. M.; Sandy, P.; Balasubramanian, S.; Mele, D. A.; Bergeron, L.; Sims, R. J. Targeting MYC dependence in cancer by inhibiting BET bromodomains. *Proc. Natl. Acad. Sci. U.S.A.* **2011**, *108*, 16669−16674.

(37) Delmore, J. E.; Issa, G. C.; Lemieux, M. E.; Rahl, P. B.; Shi, J.; Jacobs, H. M.; Kastritis, E.; Gilpatrick, T.; Paranal, R. M.; Qi, J.; Chesi, M.; Schinzel, A. C.; McKeown, M. R.; Heffernan, T. P.; Vakoc, C. R.; Bergsagel, P. L.; Ghobrial, I. M.; Richardson, P. G.; Young, R. A.; Hahn, W. C.; Anderson, K. C.; Kung, A. L.; Bradner, J. E.; Mitsiades, C. S. BET bromodomain inhibition as a therapeutic strategy to target c-Myc. *Cell* **2011**, *146*, 904−917.

(38) Srivastava, V.; Tandon, A.; Ray, S. Convenient and selective acetylations of phenols, amines and alcohols. *Synth. Commun.* **1992**, *22*, 2703−2710.